Cancer Research

RETRACTED: Differential Effects of VEGFR-1 and VEGFR-2 Inhibition on Tumor Metastases Based on Host Organ Environment

Yoon-Jin Lee[1], Daniel L. Karl[1], Ugwuji N. Maduekwe[1], Courtney Rothrock[1], Sandra Ryeom[3], Patricia A. D'Amore[2], and Sam S. Yoon[1,3]

Abstract

Tumors induce new blood vessel growth primarily from host organ microvascular endothelial cells (EC), and microvasculature differs significantly between the lung and liver. Vascular endothelial growth factor (VEGF or VEGF-A) promotion of tumor angiogenesis is thought to be mediated primarily by VEGF receptor-2 (VEGFR-2). In this study, VEGFR-2 antibody (DC101) inhibited growth of RenCa renal cell carcinoma lung metastases by 26%, whereas VEGFR-1 antibody (MF-1) had no effect. However, VEGFR-2 neutralization had no effect on RenCa liver metastases, whereas VEGFR-1 neutralization decreased RenCa liver metastases by 31%. For CT26 colon carcinoma liver metastases, inhibition of both VEGFR-1 and VEGFR-2 was required to induce growth delay. VEGFR-1 or VEGFR-2 inhibition decreased tumor burden not by preventing the establishment of micrometastases but rather by preventing vascularization and growth of micrometastases by 55% and 43%, respectively. VEGF induced greater phosphorylation of VEGFR-2 in lung ECs and of VEGFR-1 in liver ECs. EC proliferation, migration, and capillary tube formation *in vitro* were suppressed more by VEGFR-2 inhibition for lung EC and more by VEGFR-1 inhibition for liver EC. Collectively, our results indicate that liver metastases are more reliant on VEGFR-1 than lung metastases to mediate angiogenesis due to differential activity of VEGFRs on liver EC versus lung EC. Thus, therapies inhibiting specific VEGFRs should consider the targeted sites of metastatic disease. *Cancer Res; 70(21); 8357–67. ©2010 AACR.*

Introduction

Vascular endothelial growth factor (VEGF or VEGF-A) is overexpressed by the vast majority of solid tumors (1), and circulating levels of VEGF are elevated in many cancer patients, including those with colorectal and renal cell cancer (2). Inhibition of VEGF can effectively suppress tumor angiogenesis in mouse tumor models (3), and numerous inhibitors of VEGF are currently in clinical use (4). VEGF exerts its effects primarily through two tyrosine kinase receptors, VEGF receptor-1 (VEGFR-1; Flt-1) and VEGFR-2 (Flk-1, KDR), which are expressed by endothelial cells (EC; ref. 3). VEGFR-2 is believed to mediate the primary downstream effects of VEGF on ECs including increased vascular permeability, proliferation, migration, and survival (5). VEGFR-1 has generally been thought to transmit only weak mitogenic signals (6).

New tumor blood vessels are derived primarily from the microvascular ECs of the host organ or tissue (7), although there is also a contribution from bone marrow–derived EC precursors (8, 9). Significant heterogeneity exists between the microvascular endothelium of different organs in terms of structure and function (10), and ECs from different microvascular beds have distinct gene expression patterns (11) and cell surface proteins (12). Morphologically, liver (microvascular) sinusoidal ECs are discontinuous with fenestrations and allow free passage of nutrient-rich plasma, whereas lung microvascular ECs are continuous and prevent accumulation of fluid (12). The amount of VEGF produced by surrounding parenchymal cells is an essential factor in these morphologic differences (13). Given that microvascular ECs from different organs have such heterogeneous characteristics and requirements for VEGF, it is reasonable to expect that inhibitors of VEGF or VEGFRs may have significantly different effects on metastatic tumors growing in various organ sites (14).

Neutralizing antibodies targeting specifically VEGFR-1 or VEGFR-2 are currently being examined in clinical trials for metastatic solid tumors often without consideration for the specific sites of disease (15). In this study, we examined the effects of VEGFR-1 and VEGFR-2 inhibition *in vitro* on lung and liver ECs. We further examined the effects of VEGFR-1 and VEGFR-2 inhibition on lung and liver metastases using

Authors' Affiliations: [1]Department of Surgery, Massachusetts General Hospital and Harvard Medical School; [2]Schepens Eye Research Institute and Departments of Ophthalmology and Pathology, Harvard Medical School, Boston, Massachusetts; and [3]Department of Cancer Biology, University of Pennsylvania School of Medicine, Philadelphia, Pennsylvania

Note: Supplementary data for this article are available at Cancer Research Online (http://cancerres.aacrjournals.org/).

Y-J. Lee and D.L. Karl contributed equally to this work.

Current address for Y-J. Lee: Division of Radiation Effects, Korea Institute of Radiological and Medical Science, 215-4 Seoul 139-706, Korea.

Corresponding Author: Sam S. Yoon, Departments of Surgery and Cancer Biology, University of Pennsylvania School of Medicine, 4 Silverstein, 3400 Spruce Street, Philadelphia, PA 19104. Phone: 215-614-0857; Fax: 215-662-7476; E-mail: sam.yoon@uphs.upenn.edu.

doi: 10.1158/0008-5472.CAN-10-1138

two different cancer cell lines. Surprisingly, VEGFR-1 was found to play a greater role than VEGFR-2 in liver EC proliferation, migration, and capillary tube formation as well as in the vascularization of liver metastases.

Materials and Methods

Cell lines

RenCa renal carcinoma cells, CT26 mouse colon carcinoma cells, SVR mouse angiosarcoma cells, and DC101 and MF-1 hybridoma cells were obtained from the America Type Culture Collection (ATCC). MC26 mouse colon carcinoma cells were obtained from National Cancer Institute (NCI) Tumor Repository. Human umbilical vein ECs (HUVEC) were obtained from Lonza. Human liver sinusoidal ECs and human lung microvascular ECs were obtained from ScienCell. All ECs were used within eight passages. Cancer cell lines were actively passaged for <6 months from the time that they were received from ATCC or NCI Tumor Repository, and the United Kingdom Coordinating Committee on Cancer Research guidelines were followed (16). Normal mouse lung microvascular EC (m-lung EC) and mouse liver sinusoidal EC (m-liver EC) were isolated from BALB/c mice, as we have previously described (17). CT26 lung metastases were isolated 3 weeks following tail vein injection, and CT26 liver metastases were isolated 2 weeks following intrasplenic injection. ECs from metastases were isolated in a similar fashion.

DC101 and MF-1 antibodies were produced from hybridoma cells using the BD CELLine 1000 system (BD Biosciences) following the manufacturer's instructions.

In vitro EC assays

Human ECs and cancer cell lines were tested after 12 to 24 hours of incubation in Optimen with 1% fetal bovine serum (FBS) for proliferation using a colorimetric MTT assay, migration using a modified Boyden chamber, and/or capillary tube formation using Matrigel, as we have previously described (18). Recombinant human VEGF (10 ng/mL, NCI), antihuman VEGFR-1 antibody (AF321, 0.5 μg/mL, R&D Systems), antihuman VEGFR-2 antibody (MAB3572, 0.5 μg/mL, R&D Systems), recombinant murine VEGF (10 ng/mL, R&D), antimouse VEGFR-1 antibody (MF-1, 0.5 μg/mL), and/or antimouse VEGFR-2 antibody (DC101, 0.5 μg/mL) were added where indicated. Proliferation of mouse ECs and tumor ECs was assessed using a bromodeoxyuridine (BrdUrd) incorporation assay. Cells were incubated in 10 μmol/L BrdUrd (Sigma) for 12 hours. The incorporated BrdUrd was stained with anti-BrdUrd-FITC (1:50, BD Pharmingen), and a percentage of BrdUrd positive cells were examined by fluorescence-activated cell sorting (FACS).

FACS analysis

Cells were fixed in 70% ethanol and incubated with mouse anti-CD31 monoclonal antibody (mAb; 1:100; Pharmingen) for 1 hour at 4°C. Cells were then incubated with goat anti-mouse Alexa 488–conjugated secondary antibody (1:500; Molecular Probes) for 30 minutes at 4°C and analyzed with a FACScan flow cytometer (Becton Dickinson).

Western blot analysis

For Western blot analysis of VEGFRs, ECs in Optimem with 1% FBS were treated with VEGF (10 ng/mL) where indicated. VEGFR neutralizing antibodies were added where indicated 1 hour before addition of VEGF. Cells were harvested 5 minutes after VEGF administration. For normal organs and metastases, tissues were snap frozen in liquid nitrogen and thawed in radioimmunoprecipitation assay buffer containing Complete Protease Inhibitor Cocktail (Roche) and Phosphatase Inhibitor Cocktail (Sigma). DNA was sheared through a 21-gauge needle. Samples were sonicated for 10 to 20 seconds and then centrifuged at 4°C for 20 minutes at 10,000 × *g*. The supernatant was collected, and protein concentration was determined by BCA Protein Assay Kit (Pierce). Western blot analysis was performed for total and phosphorylated VEGFR-1 and VEGFR-2 using the following antibodies: phosphorylated VEGFR-1 (Tyr^{1213}, 1:20,000, Upstate), phosphorylated VEGFR-2 (Tyr^{1175}, 1:1,000, Cell Signaling), total VEGFR-1 (1:500, Santa Cruz), and total VEGFR-2 (1:1,000, Cell Signaling).

For signal transducer and activator of transcription 3 (STAT3) Western blot analyses, ECs were treated with VEGF, VEGF-E (10 ng/mL, Fitzgerald Industries), or placental growth factor (PlGF; 10 ng/mL, R&D Systems) for 7 minutes, and lysates were collected and probed for phosphorylated STAT3 (1:2,000, 9145S, Cell Signaling), total STAT3 (1:1,000, 9132, Cell Signaling), and β-actin (1:10,000; Abcam). EC and cancer cells lysates were also examined for neuropilin-1 (NRP-1) by Western blot analysis (1:1,000, Santa Cruz).

Quantitative reverse transcription–PCR

Quantitative real-time PCR analysis was performed using the LightCycler Detection System (Roche Diagnostics) as previously described (19). Primers for mouse VEGFR-1 and VEGFR-2 were the following: VEGFR-1, (forward) 5′-CGG AAG GAA GAC AGC TCA TC-3′ and (reverse) 5′-CTT CAC GCG ACA GGT GTA GA-3′; VEGFR-2, (forward) 5′-GGC GGT GGT GAC AGT ATC TT-3′ and (reverse) 5′-TCT CCG GCA AGC TCA AT-3′.

Immunohistochemical and immunofluorescence microscopy

CD31 immunohistochemical localization and analysis of microvessel density (MVD) were performed as previously described (19). For VE-cadherin and CD31 immunofluorescence, cells were fixed and incubated with rat VE-cadherin mAb (1:100, R&D Systems) and mouse anti-CD31 mAb (1:100; Pharmingen) overnight at 4°C. Following washing, sections were incubated with goat anti-rat Alexa 594 (1:500; Molecular Probes) and goat antimouse Alexa 488–conjugated secondary antibodies (1:500; Molecular Probes) for 1 hour at room temperature. Cell nuclei were labeled with Hoechst dye (1 μg/mL). For VEGFR-2 and platelet/EC adhesion molecule 1 (PECAM-1) immunofluorescence, paraffin-embedded tissue sections were incubated with goat anti-PECAM-1 (1:100, Santa Cruz

Biotechnology) and mouse anti-VEGFR2 (1:100, Santa Cruz Biotechnology) and then incubated with antigoat Alexa 488 and antimouse Alexa 594-conjugated secondary antibodies (1:500, Molecular Probes). Subsequently, tissues were stained with 4′,6-diamidino-2-phenylindole (0.2 μg/mL) for 3 minutes. Images were obtained on a Zeiss microscope and analyzed using AxioVision 4.0 software (Carl Zeiss Vision).

Mouse studies

All mouse protocols were approved by the Massachusetts General Hospital Subcommittee on Research Animal Care. To generate lung and liver metastases, 0.5–1.5 × 10^6 cells were injected into the tail vein or spleen. The following day, mice were treated with either DC101 (40 mg/kg), MF-1 (40 mg/kg), a combination of DC101 and MF-1, or isotype control IgG1s (40 mg/kg) three times per week. Lungs were harvested at 3 weeks, and livers were harvested at 2 weeks following tumor cell injection. Organs were weighed, fixed in formalin, and then photographed. To determine number and size of metastases, lungs were harvested at 14 days and livers were harvested at 8 days, fixed in formalin, and serially sectioned with 0.5 to 1 mm between sections. Two magnified fields per section and five sections per organ were examined, and metastases were counted by a masked observer. Photographs were taken of each counted field, and the area of each metastasis was determined using SPOT Advanced v4.6 software (Diagnostic Instruments, Inc.).

Statistical analysis

Groups were compared using Instant 3.10 software (GraphPad). For comparisons between more than two groups, treatment groups were compared with the control group using one-way ANOVA with Bonferroni adjustment for multiple comparisons. *P* values of <0.05 were considered significant.

Results

Differential effects of VEGFR-1 and VEGFR-2 inhibition on renal cell carcinoma metastases to the lung versus liver

To specifically assess the contributions of VEGFR-1 and VEGFR-2 activation in promoting angiogenesis in lung and liver metastases, we examined the effects of neutralizing antibodies to VEGFR-1 and/or VEGFR-2 on RenCa renal cell carcinoma liver and lung metastases in syngeneic wild-type BALB/c mice. The RenCa cell line was chosen because it expresses high levels of VEGF compared with other mouse cancer cell lines (19). MF-1 and DC101 are mAbs that bind and neutralize VEGFR-1 and VEGFR-2, respectively (20, 21). Mice were injected via tail vein with RenCa cells to generate lung metastases or into the spleen to generate liver metastases. Neutralization of VEGFR-2 with DC101 over 21 days significantly inhibited RenCa lung metastases (26% reduction in mean organ weight), whereas neutralization of VEGFR-1 with MF-1 had minimal effect (Fig. 1A and B). In contrast, blockade of VEGFR-1 with MF1 over 14 days inhibited RenCa liver metastases (31% reduction in mean organ weight), whereas blockade of VEGFR-2 with DC101 had minimal effect. Neutralization of both VEGFR-1 and VEGFR-2 with a combination of MF-1 and DC101 did not lead to additional inhibition of either lung or liver metastases. These experiments were repeated two more times with similar results.

Because VEGF signaling is known to play a role in both the establishment of metastatic lesions as well as the growth of metastases, we examined the effects of VEGFR-1 and VEGFR-2 inhibition on the number and size of metastases in the lung and liver. Mice with RenCa lung metastases were treated with neutralizing antibodies, but lungs were harvested at 14 days rather than at 21 days, and the number and size of metastases were examined in serial sections. DC101 treatment led to an appreciable decrease in the size of lung metastases (Fig. 1C) but had no effect on the mean number of lung metastases (Supplementary Fig. S1A and B). Mice with RenCa liver metastases treated with MF-1 (sacrificed at 8 days instead of 14 days) had a significant decrease in the size of liver metastases with no change in the number of liver metastases. Analysis of MVD using CD31 immunohistochemistry or PECAM immunoflurescence of lung and liver metastases, respectively, revealed that decreases in size of metastases due to MF-1 or DC101 treatment was accompanied by decreases in MVD (Fig. 1D).

Differential activation of VEGFR-1 and VEGFR-2 in lung and liver ECs

To determine if variations in VEGFR-1 and VEGFR-2 levels in different organ environments could explain differences in response to VEGFR inhibitors, we examined levels of VEGFR-1 and VEGFR-2 in normal mouse lung and liver by both quantitative reverse transcription–PCR (RT-PCR) and Western blot analysis. VEGFR-1 levels were moderately higher in lung compared with liver, and VEGFR-2 levels were roughly equivalent in lung compared with liver (Supplementary Fig. S2A and B). Thus, different levels of VEGFR-1 and VEGFR-2 in lung and liver did not account for the distinct effects of VEGFR inhibition on lung and liver metastases.

To better assess VEGFR signaling in lung and liver ECs, we next analyzed VEGFRs in lung ECs and liver ECs. Cell lysates were analyzed by Western blot analysis for total and phosphorylated VEGFR-1 and VEGFR-2 before and after the addition of VEGF. In lung EC, VEGF treatment led to phosphorylation of both VEGFR-1 and VEGFR-2 (Fig. 2A). However, in liver EC, the addition of VEGF resulted in significant phosphorylation of VEGFR-1 and only minimal phosphorylation of VEGFR-2. Phosphorylation of VEGFR-1 and VEGFR-2 were inhibited by neutralizing antibodies to these receptors. Quantification of VEGFR phosphorylation following VEGF treatment showed greater VEGFR-2 activation in lung EC and greater VEGFR-1 activation in liver EC (Fig. 2B).

To directly examine the effects of VEGFR-1 and VEGFR-2 signaling on EC function, we analyzed lung EC and liver EC in three different endothelial activation assays: proliferation, migration, and tube formation (Fig. 2C). Proliferation as measured by both lung EC and liver EC was increased in response to VEGF stimulation. Proliferation of lung EC was inhibited to a greater degree by neutralizing antibody to

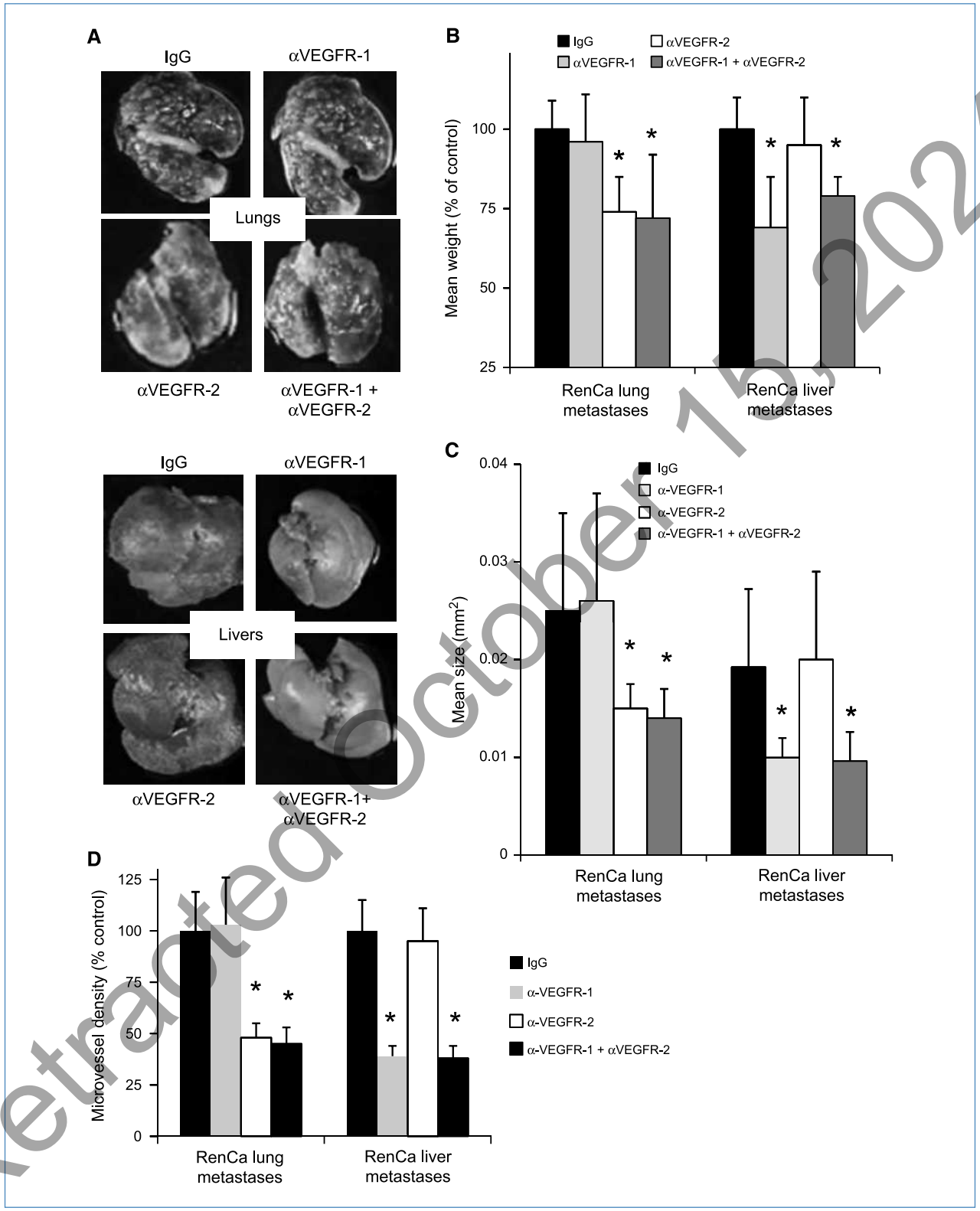

Figure 1. Differential effects of VEGFR-1 and VEGFR-2 inhibition on lung and liver metastases. A, RenCa renal carcinoma lung and liver metastases in mice treated with VEGFR antibodies MF-1 (αVEGFR-1), DC101 (αVEGFR-2), and/or control IgG (n = 6 mice per group). B, mean weight of lung and livers as percentage of control. C, mean size of RenCa metastases. D, MVD as percentage of control. Bars, SD. *, $P < 0.05$, compared with IgG control group.

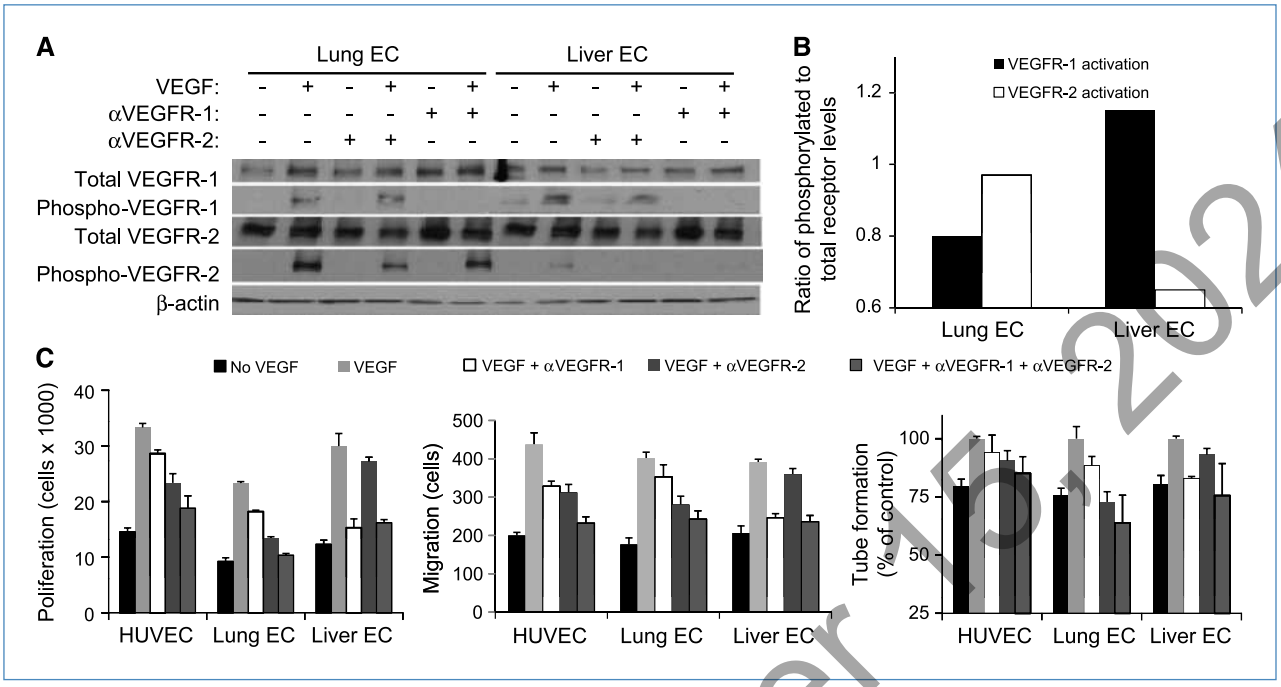

Figure 2. VEGFR-1 and VEGFR-2 expression in human lung and liver ECs and *in vitro* EC assays. A, Western blot analysis for total and phosphorylated VEGFR-1 and VEGFR-2 in lung ECs and liver EC lysates. VEGF, neutralizing antibody to VEGFR-1 (αVEGFR-1), and neutralizing antibody to VEGFR-2 (αVEGFR-2) were added where indicated. β-Actin blot serves as loading control. B, quantification of VEGFR-1 and VEGFR-2 phosphorylation relative to total VEGFR-1 and VEGFR-2 expression. C, EC proliferation (using MTT assay), migration (using modified Boyden chamber), and capillary tube formation (using Matrigel) for lung EC and liver EC. VEGF, αVEGFR-1, and/or αVEGFR-2 were added where indicated. All data are represented as a percentage with the addition of VEGF alone given a value of 100%. Bars, SD. *P* values are in text.

VEGFR-2 than by neutralizing antibody to VEGFR-1 (42% versus 22%, $P < 0.01$). In contrast, proliferation of liver EC was inhibited more by VEGFR-1 neutralizing antibody than by VEGFR-2 neutralizing antibody (49% versus 9%, $P < 0.001$). The same pattern of responses was seen when EC migration was analyzed in a modified Boyden chamber. Anti-VEGFR-2 antibody had a greater inhibitory effect for lung EC (30% versus 12%, $P < 0.01$), and anti-VEGFR-1 showed greater inhibition of liver EC migration (39% versus 10%, $P < 0.05$). Finally, for capillary tube formation on growth factor–reduced Matrigel, anti-VEGFR-2 antibody had a greater inhibitory effect on lung EC (27% versus 11%, $P < 0.01$) and anti-VEGFR-1 antibody had a greater inhibitory effect on liver EC (16% versus 7%, $P < 0.001$). Combination therapy with both anti-VEGFR-1 and anti-VEGFR-2 antibodies had an additive effect in inhibiting EC proliferation, migration, and tube formation in lung EC but had no additive effect in liver EC.

To confirm the differential effects of VEGFR-1 and VEGFR-2 inhibition on m-lung EC and m-liver EC, we isolated these cells from normal mouse lung and mouse liver. FACS analysis for CD31 before and after the second round of isolation showed significantly increased CD31 expression (Supplementary Fig. S3A). EC purity was also assessed by double labeling for VE-cadherin and CD31, and the vast majority of cells expressed both EC markers (Supplementary Fig. S3B). VEGF treatment of m-lung EC and m-liver EC led to differential activation of VEGFR-1 and VEGFR-2 similar to that seen in human liver and lung ECs. VEGF treatment in m-lung EC led to more phosphorylation of VEGFR-2 than VEGFR-1, whereas VEGF treatment of m-liver EC led to more phosphorylation of VEGFR-1 than VEGFR-2 (Fig. 3A). Similarly, inhibition of m-lung EC proliferation *in vitro* was greatest with VEGFR-2 neutralization, whereas inhibition of m-liver EC proliferation was greatest with VEGFR-1 neutralization (Fig. 3B).

Effects of VEGFR-1 and VEGFR-2 inhibition on colorectal carcinoma lung and liver metastases

To ensure that the differential effects of VEGFR-1 and VEGFR-2 inhibition against liver and lung metastases were a function of the host organ environment and not specific to the RenCa cell line, we performed similar *in vivo* metastasis experiments using CT26 colon carcinoma cells. For lung metastases, anti-VEGFR-2 therapy with DC101 significantly attenuated the growth of lung metastases (23% reduction in mean weight), but anti-VEGFR-1 therapy had minimal effect (Fig. 4A and B). The addition of MF-1 to DC101 decreased the mean weight by 33%. In contrast to lung metastases, MF-1 or DC101 alone had no effect on liver metastases and only the combination of MF-1 and DC101 inhibited liver metastases (mean weight reduction, 25%). These experiments were repeated two more times with similar results. MVD was decreased up to 55% in lung metastases treated with DC101 or a combination of MF-1 and DC101 (Fig. 4C and D). For liver metastases, treatment with MF-1 and DC101 reduced MVD by 43%.

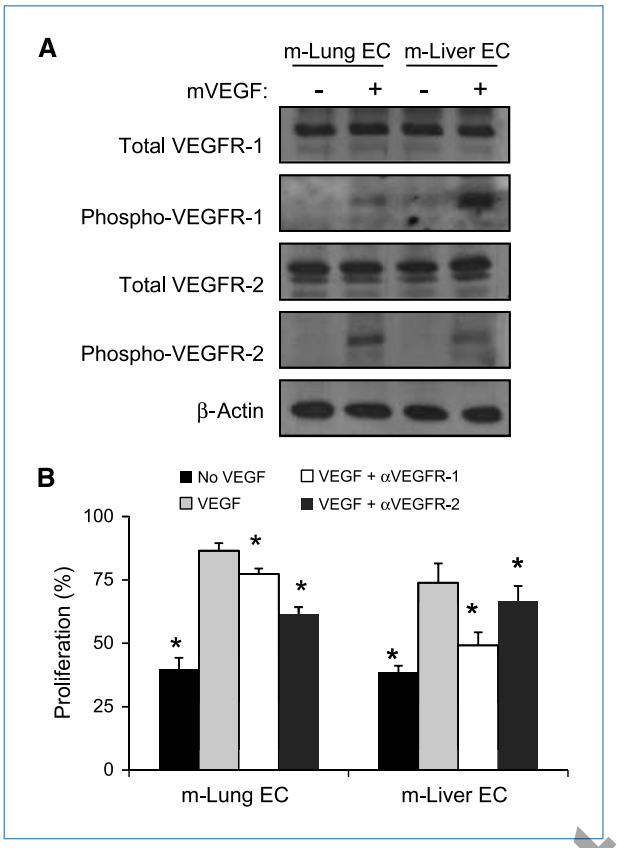

Figure 3. VEGFRs on isolated mouse lung and liver ECs. A, Western blot analysis for total and phosphorylated VEGFR-1 and VEGFR-2. Recombinant murine VEGF (mVEGF) was added where indicated. β-Actin blot serves as loading control. B, EC proliferation (using BrdUrd incorporation). VEGF, αVEGFR-1, and/or αVEGFR-2 were added where indicated. All data are represented as a percentage with the addition of VEGF alone given a value of 100%. Bars, SD. *, $P < 0.05$, compared with VEGF group.

VEGFR-1 and VEGFR-2 activation in cancer cells

Some cancer cells have been reported to express VEGFRs, and inhibition of these receptors can have cancer cell autonomous effects (22). To ensure that the results observed in our *in vivo* studies were due to effects on ECs and not on the cancer cells, we examined the effect of VEGFR-1 and VEGFR-2 inhibition on CT26 and RenCa *in vitro*. Western blot analysis revealed VEGFR-1 expression, but not VEGFR-2 expression, by CT26 and RenCa cells (Fig. 5A). These results were confirmed by quantitative RT-PCR (Supplementary Fig. S2C). VEGF treatment led to VEGFR-1 phosphorylation on both cell types (Fig. 5B) but had no effect on CT26 or RenCa proliferation (Fig. 5C). VEGF led to a significant increase in CT26 migration; this increase was small when compared with migration toward 10% serum, and this increase was not inhibited by anti-VEGFR-1 antibody. VEGF had no effect on RenCa migration (Fig. 5D). To examine other possible VEGFRs that may mediate CT26 migration toward VEGF, we examined levels of NRP-1 in CT26 (and RenCa) cells and found NRP-1 to be present but at low levels compared with HUVEC or SVR mouse angiosarcoma cells (Supplementary Fig. S2C and D).

VEGF and VEGFRs in ECs isolated from metastases

In the CT26 lung and liver metastasis models, inhibition of VEGFRs transiently blocked the growth of metastases, but even with continuous treatment, metastases eventually grew to lethal sizes (data not shown). We next compared the expression of VEGFRs in CT26 lung metastases compared with normal mouse lung and found that VEGFR-1 levels remained similar whereas VEGFR-2 levels were significantly lower in lung metastases compared with normal lung (Supplementary Fig. S4A). To specifically investigate tumor versus normal ECs, ECs were next isolated from CT26 lung metastases and normal mouse lung (Supplementary Fig. S4B). Mouse lung EC grew *in vitro* as elongated, spindle-shaped cells, whereas EC isolated from lung metastases appeared more rounded (Supplementary Fig. S4C). Western blot analysis showed that VEGFR-1 levels were similar in the two EC types, but that VEGFR-2 levels were significantly reduced in lung metastasis EC compared with normal lung EC (Fig. 6A). Furthermore, VEGF treatment of normal lung ECs led to VEGFR-2 phosphorylation, whereas VEGFR-2 phosphorylation was not detectable in lung metastasis EC. Normal lung ECs showed significant proliferation in response to VEGF treatment (as assessed by BrdUrd incorporation) that was inhibited by VEGFR-2 neutralizing antibody (Fig. 6B). In contrast, ECs derived from lung metastases showed a minimal increase in proliferation in response to VEGF and minimal response to VEGFR-2 inhibition.

Using Western blot analysis, CT26 liver metastases examined were found to have lower levels of VEGFR-2 compared with normal liver, whereas levels of VEGFR-1 were equivalent (data not shown). A decrease in VEGFR-2 expression in the vasculature of liver metastases compared with the vasculature of normal liver was confirmed using coimmunofluorescence for VEGFR-2 and PECAM-1 (Supplementary Fig. S4D). ECs isolated from CT26 liver metastases were compared with those isolated from normal liver. VEGFR-1 expression was similar in both EC types (Fig. 6C). After treatment with VEGF, VEGFR-1 was less phosphorylated in liver metastases EC compared with normal liver EC. As shown previously, normal liver ECs showed increased proliferation in response to VEGF, and this proliferation was significantly reduced by anti-VEGFR-1 antibody (Fig. 6D). In contrast, the proliferation of liver metastasis ECs was only modestly stimulated by VEGF, and this proliferation was minimally inhibited by anti-VEGFR-1 antibody.

Discussion

Varying dependence on VEGFR-1 versus VEGFR-2 during tumorigenesis in different host organ environments has not been well characterized. This study was initiated following an unexpected finding in a mouse model with a targeted deletion of the calcineurin inhibitor *Dscr1*, which causes a defect in VEGFR-2 signaling and delayed growth of flank xenografts (17). When experimental lung and liver metastases were generated in these mice, the growth of lung metastases was inhibited but the growth of liver metastases was not (Supplementary Fig. S5). We thus hypothesized that VEGFR-1

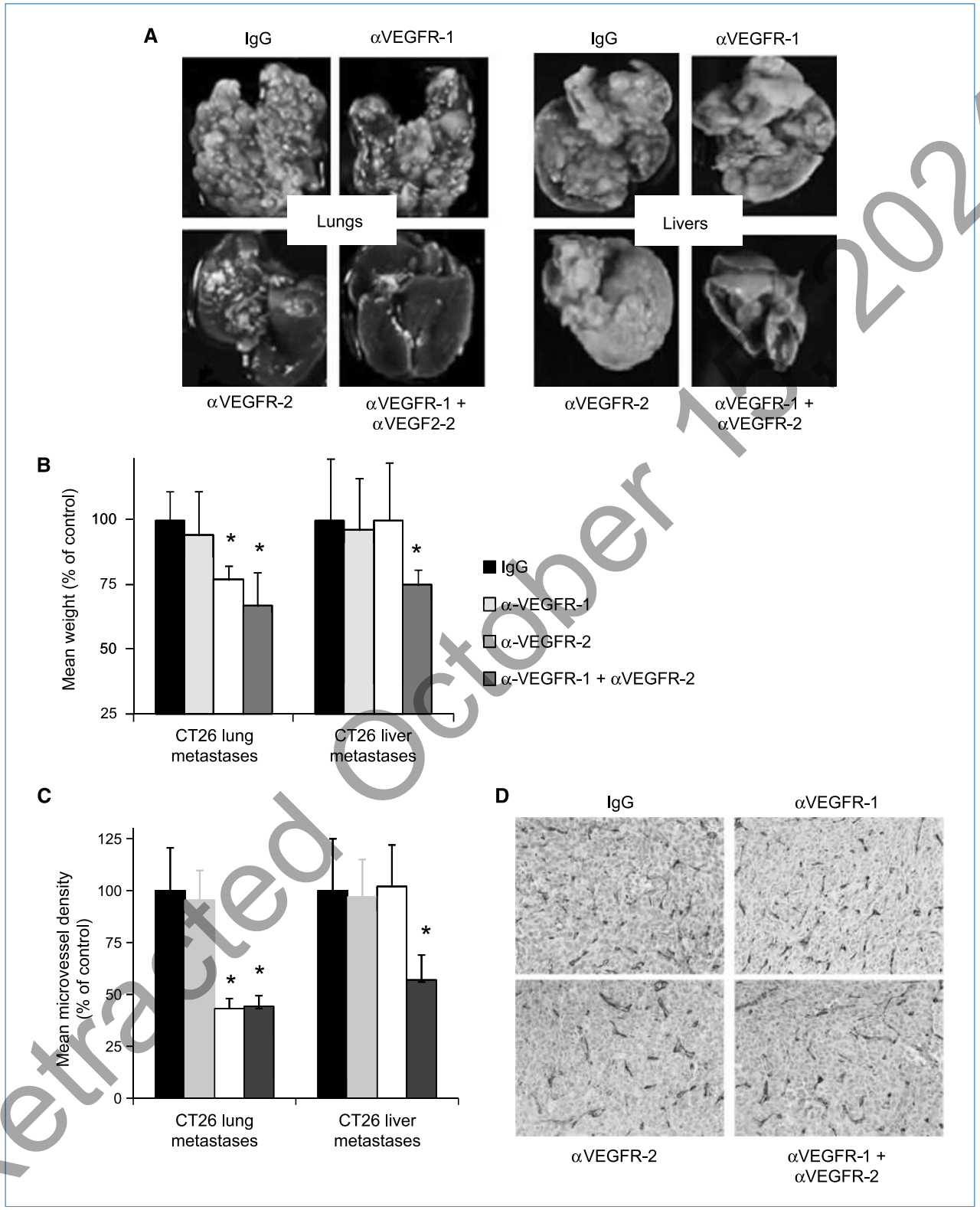

Figure 4. Effect of VEGFR-1 and VEGFR-2 neutralization on CT26 colon carcinoma lung and liver metastases. A, CT26 lung and liver metastases treated with VEGFR antibodies MF-1, DC101, or control IgG (n = 6 mice per group). B, mean weight of lung and livers as percentage of control. C, mean MVD of lung and liver metastases as percentage of control. Bars, SD. *, $P < 0.05$, compared with IgG control group. D, representative images following CD31 immunohistochemistry of lung metastases from designated treatment groups.

signaling may play a significant role in the vascularization of liver metastases. Using neutralizing antibodies specific for VEGFR-1 and VEGFR-2, we found that blockade of VEGFR-1 alone was sufficient to delay growth of RenCa liver metastases, whereas blockade of both VEGFR-1 and VEGFR-2 was required to delay growth of CT26 liver metastases. Furthermore, *in vitro* analyses of ECs from human and murine lungs and livers revealed that liver ECs have more phosphorylation of VEGFR-1 than VEGFR-2 in response to VEGF and that VEGFR-1 inhibition was more effective in blocking VEGF-induced liver EC functions. Finally, analysis of ECs isolated from metastases compared with normal tissues suggested that downregulation of VEGFRs and/or independence from VEGF-mediated proliferation may account for resistance to VEGFR inhibitors.

Several studies have examined organ-specific differences in VEGFR-1 and VEGFR-2 signaling in liver and lung development and regeneration. It has been reported that activation of VEGFR-1 in liver ECs led to the production of factors that protected the liver parenchyma from injury and initiated liver regeneration (23). In another study, VEGFR-2 inhibition had only a minor effect on liver regeneration in mice following partial hepatectomy; VEGFR-1 inhibition was not examined (24). Using a transgenic mouse expressing a luciferase reporter gene under the control of the VEGFR-2 promoter, the highest level of VEGFR-2 activity was found in the lung (25). Blockade of VEGFR-2 signaling in the perinatal period disrupted lung development in mice, whereas VEGFR-1 blockade had no effect (26). Our observation of differences in the efficacy of VEGFR inhibitors for lung and liver metastases are consistent with these reported organ-specific differences.

Numerous VEGF pathway inhibitors are currently in clinical use for patients with metastatic disease from solid tumors. Some of these therapies, such as bevacizumab (an anti-VEGF antibody), are effective as single agents against highly vascular metastases, such as those from renal cell cancer (27). Bevacizumab is also effective when combined with chemotherapy for metastases for less vascular tumors, such as colorectal cancer (28). The majority of the effects of bevacizumab against metastases have previously been thought of as a result of the inhibition of VEGFR-2 signaling (29), and specific VEGFR-2 inhibitors are currently in clinical trials (30). However, preclinical testing of new antiangiogenic

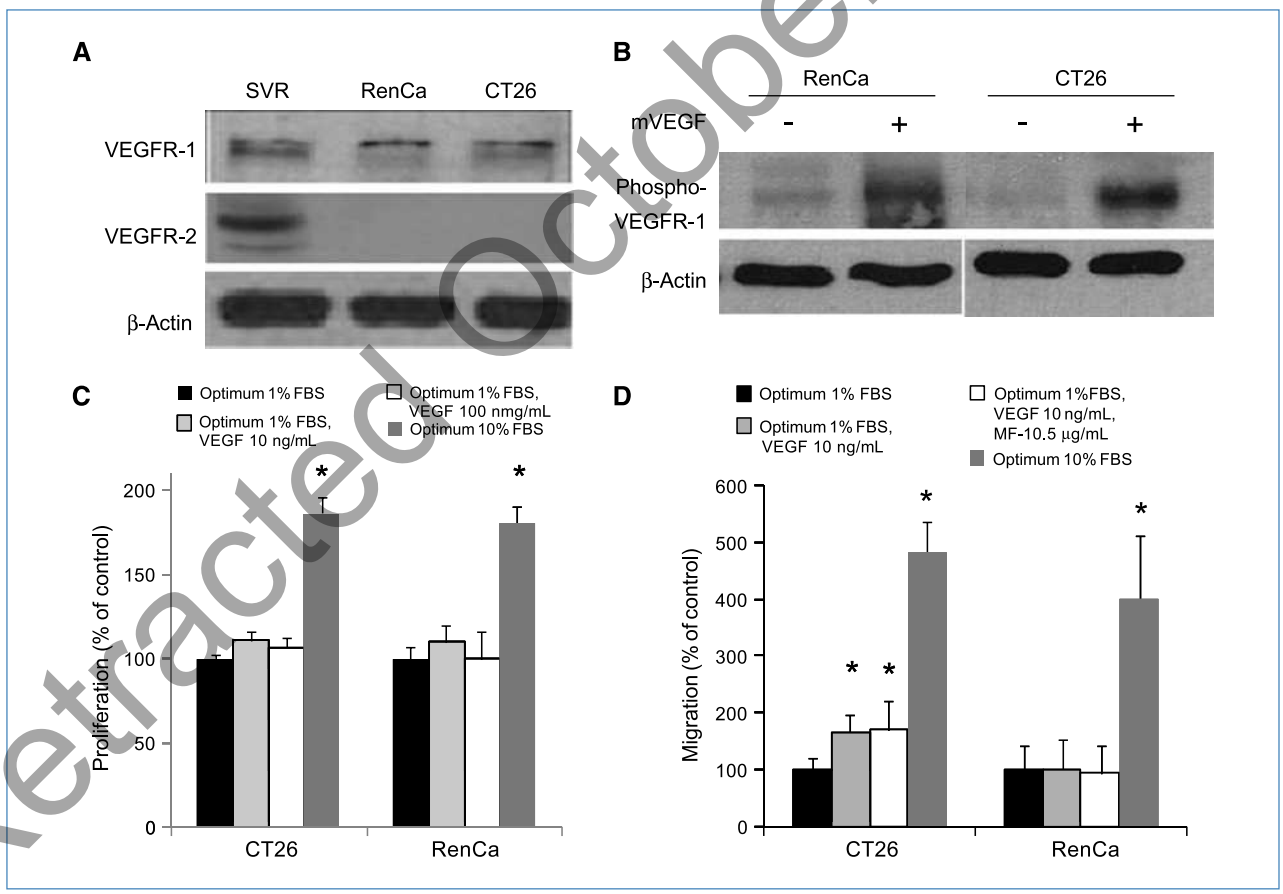

Figure 5. VEGFR expressions by cancer cells. A, Western blot analysis for VEGFR-1 and VEGFR-2 in RenCa and CT26 cell lysates. SVR is a transformed murine EC line, and this cell lysate serves as a positive control. B, Western blot analysis for phosphorylated VEGFR-1 in RenCa and CT26 cells with and without addition of mVEGF (10 ng/mL). β-Actin blots serve as loading controls. C, proliferation of CT26 and RenCa cells in response to mVEGF or 10% FBS. D, migration of CT26 and RenCa cells toward mVEGF or 10% FBS. Anti-VEGFR-1 antibody (MF-1, 0.5 μg/mL) was added where indicated.

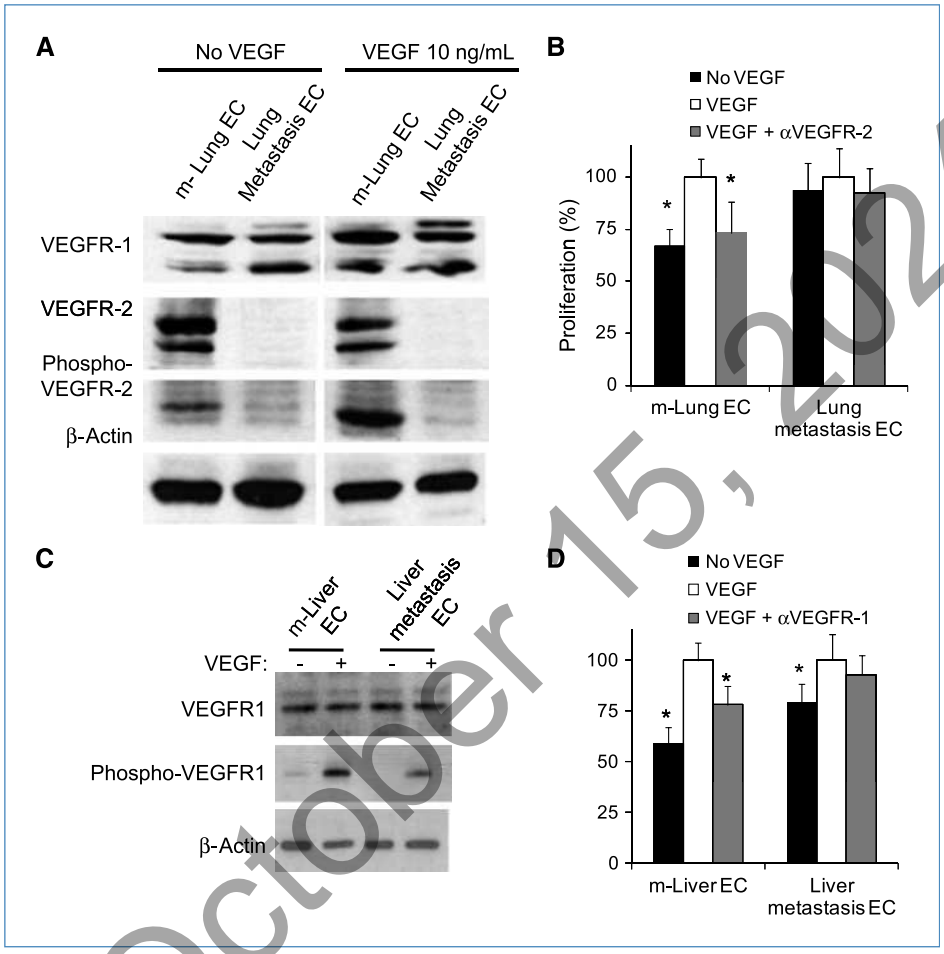

Figure 6. Tumor ECs with VEGFR downregulation and VEGF-independent growth. A, Western blots for total VEGFR-1, total VEGFR-2, and phosphorylated VEGFR-2 before and after mVEGF treatment for m-lung EC, CT26 lung metastasis ECs (lung metastasis EC), and CT26 cells. β-Actin blot serves as loading control. B, proliferation of m-lung EC and lung metastasis EC as measured by BrdUrd incorporation. C, Western blots for total VEGFR-1 and phosphorylated VEGFR-1 for m-liver ECs and CT26 liver metastasis ECs (liver metastasis EC) before and after treatment with mVEGF. D, proliferation of m-liver EC and liver metastasis EC as measured by BrdUrd incorporation. Murine VEGF (10 ng/mL), αVEGFR-1 (MF-1, 0.5 μg/mL), and αVEGFR-2 (DC101, 0.5 μg/mL) were added where indicated. All data are represented as a percentage with the addition of mVEGF alone given a value of 100%. Bars, SD. *, $P < 0.05$.

agents does not often include examination of metastases in multiple different organ environments, and this is the first study to examine the effects of VEGFR-1 and VEGFR-2 inhibition against ECs from different host organs and against metastases in different host organs.

Both CT26 and RenCa cells express VEGFR-1, and VEGF may promote CT26 migration *in vivo*. However, the disparate effects of VEGFR-1 inhibition in the liver and lung are unlikely due to the effects of VEGFR-1 inhibition on cancer cells given it had no effect on CT26 migration. Moreover, the differential effect of VEGFR-1 inhibition against metastases in the liver and lung environments was also observed for RenCa cells, whose proliferation or migration is unaffected by VEGFR-1 inhibition. CT26 and RenCa liver metastases responded differently to VEGFR inhibition; RenCa cells responded to neutralization of only VEGFR-1 whereas CT26 cells required blockage of both VEGFR-1 and VEGFR-2. The relatively higher levels of VEGF secreted by RenCa may select for VEGF-dependent EC growth, which may sensitize these metastases to VEGFR inhibition to a greater extent than CT26 metastases.

There are a variety of mechanisms by which tumors may escape angiogenesis inhibition, including upregulation of alternative angiogenic factors and pathways, development of established/mature tumor vasculature, and co-option of neighboring normal vasculature (31). It has been shown that blocking VEGFR-2 in a transgenic model of spontaneous pancreatic islet tumors led to an increase in hypoxia and upregulation not only of VEGF but also of the basic fibroblast growth factor, angiopoietin 1 and other angiogenic factors (32). We previously found that the profile of proangiogenic factors upregulated in response to overexpression of endogenous angiogenesis inhibitors varied among different tumor types (19). In this study, we further find that ECs in lung and liver metastases exhibit reduced expression of VEGFRs and/or adopt mechanisms for VEGF-independent growth. We would postulate that the bulk of the inhibitory effect of VEGFR-1 or VEGFR-2 antibody on metastases occurs in the initial vascularization of microscopic metastases from normal liver or lung ECs and that macroscopic metastases and tumor ECs become dependent on non-VEGF pathways to induce angiogenesis.

There are several possible explanations why VEGFR-1 plays a more prominent role in liver EC function and liver metastases, whereas VEGFR-2 plays a more prominent role in lung EC function and lung metastases. For example, the interaction of VEGFR-1 and VEGFR-2 in activating intracellular signaling pathways such as STAT3 (33) may vary in liver

EC versus lung EC. Using the VEGFR-1–specific ligand PlGF and the VEGFR-2 specific ligand VEGF-E, we found that PlGF activated STAT3 more in liver EC than in lung EC and that VEGF-E (compared with VEGF-A) activated STAT3 more in lung EC than in liver EC (Supplementary Fig. S6). Our studies used experimental metastasis models and not spontaneous metastasis models. The primary rationale for the use of experimental metastasis models was to examine the effects of VEGFR-1 and VEGFR-2 inhibition on established micrometastatic disease. The vast majority of patients receiving inhibitors of VEGF signaling have established metastatic diseases. The use of spontaneous metastasis models would need to account for the effects of VEGFR inhibition on both the primary tumor and developing metastases, and it may be difficult to separate these two effects. In addition, the trafficking of bone marrow–derived cells (BMDC), some of which express VEGFRs, into the tumor microenvironment, may differ between lung and liver metastases, and effects on VEGFR-1 inhibition on BMDCs may contribute to the inhibition of liver metastases (34). However, our analysis of liver ECs *in vitro* identifies VEGFR-1 as an important receptor for proliferation, migration, and tube formation.

Thus, the activity of VEGFR-1 and VEGFR-2 neutralizing antibodies against metastases varies based on host organ environment. Knowing that there is significant heterogeneity among ECs in various microvascular beds, it is logical that the effects of VEGFR inhibition against metastases in various locations may differ. As specific VEGFR-targeted agents move forward into clinical trials for the treatment and possibly prevention of tumors and metastases, differences in the activity and efficacy of these agents in various organ environments should be considered.

Disclosure of Potential Conflicts of Interest

No potential conflicts of interest were disclosed.

Grant Support

NIH grants 5 K12 CA 87723-03 and 1 R21 CA117129-01 (S.S. Yoon). P.A. D'Amore is a Research to Prevent Blindness Senior Scientific Investigator.

The costs of publication of this article were defrayed in part by the payment of page charges. This article must therefore be hereby marked *advertisement* in accordance with 18 U.S.C. Section 1734 solely to indicate this fact.

Received 04/01/2010; revised 08/02/2010; accepted 08/22/2010; published OnlineFirst 10/26/2010.

References

1. Dvorak HF. Vascular permeability factor/vascular endothelial growth factor: a critical cytokine in tumor angiogenesis and a potential target for diagnosis and therapy. J Clin Oncol 2002;20:4368–80.
2. Poon RT, Fan ST, Wong J. Clinical implications of circulating angiogenic factors in cancer patients. J Clin Oncol 2001;19:1207–25.
3. Ferrara N. The role of vascular endothelial growth factor in angiogenesis. In: Voest EE, D'Amore PA, editors. Tumor Angiogenesis and Microcirculation. New York: Marcel Dekkar, Inc.; 2001, p. 361–74.
4. Herbst RS. Therapeutic options to target angiogenesis in human malignancies. Expert Opin Emerg Drugs 2006;11:635–50.
5. Hicklin DJ, Ellis LM. Role of the vascular endothelial growth factor pathway in tumor growth and angiogenesis. J Clin Oncol 2005;23:1011–27.
6. Carmeliet P, Moons L, Luttun A, et al. Synergism between vascular endothelial growth factor and placental growth factor contributes to angiogenesis and plasma extravasation in pathological conditions. Nat Med 2001;7:575–83.
7. Fidler IJ, Ellis LM. The implications of angiogenesis for the biology and therapy of cancer metastasis. Cell 1994;79:185–8.
8. Peters BA, Diaz LA, Polyak K, et al. Contribution of bone marrow-derived endothelial cells to human tumor vasculature. Nat Med 2005;11:261–2.
9. Rafii S. Circulating endothelial precursors: mystery, reality, and promise. J Clin Invest 2000;105:17–9.
10. Aird WC. Endothelial cell heterogeneity. Crit Care Med 2003;31:S221–30.
11. Seaman S, Stevens J, Yang MY, Logsdon D, Graff-Cherry C, St Croix B. Genes that distinguish physiological and pathological angiogenesis. Cancer Cell 2007;11:539–54.
12. Pasqualini R, Arap W, McDonald DM. Probing the structural and molecular diversity of tumor vasculature. Trends Mol Med 2002;8:563–71.
13. Maharaj AS, Saint-Geniez M, Maldonado AE, D'Amore PA. Vascular endothelial growth factor localization in the adult. Am J Pathol 2006;168:639–48.
14. Conway EM, Carmeliet P. The diversity of endothelial cells: a challenge for therapeutic angiogenesis. Genome Biol 2004;5:207.
15. Spratlin JL, Cohen RB, Eadens M, et al. Phase I pharmacologic and biological study of ramucirumab (IMC-1121B), a fully human immunoglobulin G1 monoclonal antibody targeting the vascular endothelial growth factor receptor-2. J Clin Oncol 2010;28:780–7.
16. UKCCCR guidelines for the use of cell lines in cancer research. Br J Cancer 2000;82:1495–509.
17. Ryeom S, Baek KH, Rioth MJ, et al. Targeted deletion of the calcineurin inhibitor DSCR1 suppresses tumor growth. Cancer Cell 2008;13:420–31.
18. Detwiller KY, Fernando NT, Segal NH, Ryeom SW, D'Amore PA, Yoon SS. Analysis of hypoxia-related gene expression in sarcomas and effect of hypoxia on RNA interference of vascular endothelial cell growth factor A. Cancer Res 2005;65:5881–9.
19. Fernando NT, Koch M, Rothrock C, et al. Tumor escape from endogenous, extracellular matrix-associated angiogenesis inhibitors by up-regulation of multiple proangiogenic factors. Clin Cancer Res 2008;14:1529–39.
20. Hicklin DJ, Witte L, Zhu Z, et al. Monoclonal antibody strategies to block angiogenesis. Drug Discov Today 2001;6:517–28.
21. Witte L, Hicklin DJ, Zhu Z, et al. Monoclonal antibodies targeting the VEGF receptor-2 (Flk1/KDR) as an anti-angiogenic therapeutic strategy. Cancer Metastasis Rev 1998;17:155–61.
22. Dallas NA, Fan F, Gray MJ, et al. Functional significance of vascular endothelial growth factor receptors on gastrointestinal cancer cells. Cancer Metastasis Rev 2007;26:433–41.
23. LeCouter J, Kowalski J, Foster J, et al. Identification of an angiogenic mitogen selective for endocrine gland endothelium. Nature 2001;412:877–84.
24. Van BG, Yang AD, Dallas NA, et al. Effect of molecular therapeutics on liver regeneration in a murine model. J Clin Oncol 2008;26:1836–42.
25. Zhang N, Fang Z, Contag PR, Purchio AF, West DB. Tracking angiogenesis induced by skin wounding and contact hypersensitivity using a Vegfr2-luciferase transgenic mouse. Blood 2004;103:617–26.
26. McGrath-Morrow SA, Cho C, Cho C, Zhen L, Hicklin DJ, Tuder RM. Vascular endothelial growth factor receptor 2 blockade disrupts postnatal lung development. Am J Respir Cell Mol Biol 2005;32:420–7.

27. Yang JC, Haworth L, Sherry RM, et al. A randomized trial of bevacizumab, an anti-vascular endothelial growth factor antibody, for metastatic renal cancer. N Engl J Med 2003;349:427–34.
28. Ferrara N, Hillan KJ, Novotny W. Bevacizumab (Avastin), a humanized anti-VEGF monoclonal antibody for cancer therapy. Biochem Biophys Res Commun 2005;333:328–35.
29. Yancopoulos GD, Davis S, Gale NW, Rudge JS, Wiegand SJ, Holash J. Vascular-specific growth factors and blood vessel formation. Nature 2000;407:242–8.
30. Krupitskaya Y, Wakelee HA. Ramucirumab, a fully human mAb to the transmembrane signaling tyrosine kinase VEGFR-2 for the potential treatment of cancer. Curr Opin Investig Drugs 2009;10:597–605.
31. Bergers G, Hanahan D. Modes of resistance to anti-angiogenic therapy. Nat Rev Cancer 2008;8:592–603.
32. Casanovas O, Hicklin DJ, Bergers G, Hanahan D. Drug resistance by evasion of antiangiogenic targeting of VEGF signaling in late-stage pancreatic islet tumors. Cancer Cell 2005;8:299–309.
33. Chen SH, Murphy DA, Lassoued W, Thurston G, Feldman MD, Lee WM. Activated STAT3 is a mediator and biomarker of VEGF endothelial activation. Cancer Biol Ther 2008;7:1994–2003.
34. Gao D, Nolan D, McDonnell K, et al. Bone marrow-derived endothelial progenitor cells contribute to the angiogenic switch in tumor growth and metastatic progression. Biochim Biophys Acta 2009; 1796:33–40.